ANL/ET/CP-91233
CONF-9610202--

Predictions of Structural Integrity of Steam Generator Tubes Under Normal Operating, Accident, and Severe Accident Conditions*

by

Saurin Majumdar

Argonne National Laboratory
Argonne, IL 60439

September 1996

INVITED PAPER to be presented at the 24th Water Reactor Safety Meeting, October 21-23, 1996 at Bethesda, MD.

*Work supported by the Office of Nuclear Regulatory Research, U.S. Nuclear Regulatory Commission.

DISCLAIMER

Portions of this document may be illegible in electronic image products. Images are produced from the best available original document.

DISCLAIMER

Predictions of Structural Integrity of Steam Generator Tubes Under Normal Operating, Accident, and Severe Accident Conditions

Saurin Majumdar
Argonne National Laboratory
Argonne, Illinois 60439

Abstract

Available models for predicting failure of flawed and unflawed steam generator tubes under normal operating, accident, and severe accident conditions are reviewed. Tests conducted in the past, though limited, tended to show that the earlier flow-stress model for part-through-wall axial cracks overestimated the damaging influence of deep cracks. This observation is confirmed by further tests at high temperatures as well as by finite element analysis. A modified correlation for deep cracks can correct this shortcoming of the model. Recent tests have shown that lateral restraint can significantly increase the failure pressure of tubes with unsymmetrical circumferential cracks. This observation is confirmed by finite element analysis. The rate-independent flow stress models that are successful at low temperatures cannot predict the rate sensitive failure behavior of steam generator tubes at high temperatures. Therefore, a creep rupture model for predicting failure is developed and validated by tests under varying temperature and pressure loading expected during severe accidents.

Introduction

Under normal operating conditions, the pressure across a PWR steam generator tube wall, Δp_{no}, is $\approx$ 9 MPa (1300 psi); under a main steamline break (MSLB) in which the secondary side has dropped to atmospheric pressure, the pressure across the tube wall, Δp_{MSLB}, is $\approx$18 MPa (2560 psi). Tubes must actually be capable of withstanding $3 \cdot \Delta p_{no} \approx$27 MPa (3900 psi) and $1.4 \cdot \Delta p_{MSLB} \approx$25 MPa (3660 psi) to meet ASME Code and NRC requirements for sufficient design margin. The margin is lower for the MSLB because it is such an unlikely event ($\approx 10^{-5}$/reactor yr. is the usual estimated occurrence frequency). These maximum pressure capabilities are based on rupture or burst of unflawed tubes. For typical unflawed steam generator tubes made of Alloy 600, the burst pressure, p_b, is $\approx$ 65 MPa (9400 psi).

Although the design of steam generator tubes are conducted assuming that the tubes are unflawed or without defects, operating experience with PWR steam generators both in the US and abroad has shown that cracks of various morphology can and do occur in the steam generator tubes starting very early in life. These cracks may be axial or circumferential, ID or OD initiated, part-through-wall or through-wall, single or multiple which may be parallel or form a network of cracks. Tests have shown that, depending on the location and morphology of these cracks, the steam generator tubes can be weakened to various extents. A purpose of the design margins is to cover such losses in strength due to service-induced defects. However, because of the potential for containment bypass with resulting release of radioactivity to the public, both rupture and/or leakage of the steam generator tubes during normal operations and accident conditions are of concern to the NRC. To evaluate the risks posed by such events, models for predicting such rupture and leakage are needed.

There is a substantial literature[1-6] on the development and validation of analytical models to describe the behavior of flawed tubes at normal reactor operating temperatures (288–320°C). These models and data can be used to analyze the potential for rupture during design basis accidents, during which the temperature of the steam generator tubing is less than 350°C. In this temperature range, creep effects are negligible in Alloy 600. However, in severe accidents[7-8], much higher temperatures are possible. At these higher temperatures, plastic deformation is likely to be much more extensive than at normal reactor operating temperatures, and creep effects can no longer be neglected. Currently, there exist no test data or validated models to predict the failure of flawed tubes at temperatures associated with severe accidents. Therefore, the NRC has initiated a program at ANL to generate failure data on flawed and unflawed steam generator tubes at high temperatures. A creep rupture model for failure of the remaining ligament of a part-through crack has been developed and validated by tests on tubes containing axial cracks.

All the analytical models discussed in this paper are applicable to steam generator tubes containing a single dominant crack. Although there has been some limited analytical and experimental studies of failure of tubes containing multiple cracks, the current practice is to be conservative and apply the existing models to a single enveloping crack.

Low temperature failure of tubes

Axial cracks

The critical pressures and crack sizes for the unstable rupture (burst) of a thin-wall internally pressurized cylindrical shell with a single through-wall axial crack can be estimated using an equation, originally proposed by Hahn et al.[1] and later modified by Erdogan[2]:

$$p_{cr} = \frac{\bar{\sigma} h}{m R_m} = \frac{p_b}{m} \tag{1a}$$

where

$$\bar{\sigma} = \text{ flow stress } = k(\sigma_y + \sigma_u) \quad (\text{with } k = 0.5 - 0.6), \tag{1b}$$

σ_y and σ_u are the yield and ultimate tensile strengths, respectively, (1c)

$$m = 0.614 + 0.481\lambda + 0.386\exp(-1.25\lambda), \tag{1d}$$

$$\lambda = \left[12(1-\nu^2)\right]^{\frac{1}{4}} \frac{c}{\sqrt{R_m h}} = \frac{1.82c}{\sqrt{R_m h}}, \tag{1e}$$

$$p_b = \frac{\bar{\sigma} h}{R_m} = \text{burst pressure of an unflawed virgin tubing}, \tag{1f}$$

R_m and h= mean radius and wall thickness of tube, respectively, (1g)

and

2c= axial crack length. (1h)

For a single part-through axial crack, the pressure required to rupture the remaining ligament can be calculated using an empirical equation (referred to as the BCL equation) reported by Kiefner et al.[4]

$$p_{sc} = \frac{\bar{\sigma} h}{m_p R_m} = \frac{p_b}{m_p} \tag{2a}$$

where

$$m_p = \frac{1 - \frac{a}{mh}}{1 - \frac{a}{h}}, \tag{2b}$$

and

a = axial crack depth

Under the auspices of an NRC sponsored steam generator integrity program, PNNL[6] conducted a series of tests on tubes containing part–through axial cracks. Based on these tests, PNNL[6] developed an empirical formula for the failure pressure of a tube containing a part–through axial crack, which is of the same form as Eq. 2a but where Eq. 2b is replaced by:

$$m_p = \left[1 - \frac{a}{h} + \frac{a}{h}\exp(-0.41\lambda)\right]^{-1} \tag{3a}$$

Chavez et al.[9] re-analyzed the PNNL tube test data and proposed that the value of k in Eq. 1b should be taken as 0.5973 and that Eq. 3a should be modified (referred to as the INEL equation) to:

$$m_p = \left[1 - \frac{a}{h} + \frac{a}{h}\exp(-0.51\lambda)\right]^{-1} \tag{3b}$$

As the crack depth approaches 100% of the thickness (i.e., a/h=1), Eqs. 2a-2b predict that p_{sc} approaches 0 while Eqs. 3a and 3b do not predict that p_{sc} approaches 0, i.e., they predict higher pressure for ligament rupture than Eqs. 2a-2b for short, deep cracks. Eventually Eqs. 3a-3b should become unconservative for very deep cracks. On the other hand, Eq. 2a tends to be overly conservative for short and deep cracks. Therefore, Shack[10] has re-analyzed the PNNL tube test data and proposed that Eq. 2b be modified as follows (referred to as the ANL equation):

$$m_p = \frac{1 - \alpha\left(\frac{a}{h}\right)\frac{a}{mh}}{1 - \frac{a}{h}} \tag{2c}$$

$$\text{where } \alpha\left(\frac{a}{h}\right) = 1 + 0.94\left(\frac{a}{h}\right)^2\left[1 - \frac{1}{m}\right]$$

Except for short and deep cracks, Eq. 2c predicts similar rupture pressures as Eq. 2b.

Based on burst tests on tubes, Flesch and Cochet[5] recommended the use of Eqs. 2a-b for flaw depths greater than 85% of the wall thickness. However, in order to reduce the degree of conservativeness, they used σ_u instead of $\overline{\sigma}$. For predicting failure of the remaining ligament by plastic instability of tubes with flaw depths between 20% and 85% of wall thickness, they recommended replacing Eq. 2b by the following empirical equation (referred to as the EDF equation):

$$m_p = \left[1 - \frac{\frac{c}{h}\frac{a}{h}}{1 + \frac{c}{h}}\right]^{-1} \quad \text{for } 0.2 < a/h < 0.85 \tag{4a}$$

and

$$m_p = \frac{1-\frac{a}{mh}}{1-\frac{a}{h}}\frac{\overline{\sigma}}{\sigma_u} \text{ for } a/h > 0.85 \tag{4b}$$

It should be emphasized that Eq. (2a) gives only the pressure required to rupture the remaining ligament. The stability of the resulting throughwall crack can be analyzed using Eq. (1a). If $p_{cr} > p_{sc}$, the throughwall crack is stable. Although the crack will leak, it will not increase in length without a further increase in pressure. If $p_{cr} < p_{sc}$, the resulting crack will be unstable and will rapidly increase in length without any additional increase in pressure.

A comparison of the values of stress magnification factor m_p as computed by the various equations is shown in Figs. (1a-b). Note that although the values of m_p as computed by the various equations are within 20-30% of each other for a shallow crack (a/h=0.5), they can differ by as much as a factor of 2 for deep (a/h=0.9) and short cracks (~0.25 in.). Rupture tests on tubes containing deep cracks (to be discussed later) have shown that the m_p values are more in accordance with the ANL equation (Eq. 2c) than the BCL equation (Eq. 2b). To verify this analytically, detailed elastoplastic finite-element analyses were conducted for a 22 mm (7/8 in.) diameter tube with a 25 mm (1 in.) long and 50% deep axial crack and a 6 mm (0.25 in.) long and 90% deep axial crack subjected to rapidly increasing internal pressure at 300°C and 750°C. The stress-strain curves at these temperatures are shown in fig. 2a. Results, presented in fig. 2b, show that the maximum hoop stress magnification in the ligament for the shallower crack is independent of the stress-strain curve of the material. Further, the hoop stress magnification factor (defined as the ratio of the average hoop stress in the ligament and the average hoop stress in an unflawed tube) changes very little with internal pressure and its variation with crack depth is more in agreement with the ANL equation than the BCL equation.

Circumferential cracks

Failure loads for tubing with circumferential cracks can also be calculated using plastic limit load analyses described by Ranganath et al.[11] which were based on earlier work by Kanninen et al.[12] For an unconstrained tube with a throughwall crack of angular length 2θ and no applied primary bending stress, the critical burst pressure is

$$p_{cr} = \frac{2\overline{\sigma}h}{R_m}\left(1-\frac{\theta}{\pi}-\frac{2\beta}{\pi}\right) \tag{5a}$$

where

$$\beta = \sin^{-1}\left(\frac{\sin\theta}{2}\right) \tag{5b}$$

Limit load analyses have also been proposed for part–through cracks.[13-14]

Eq. 5a is applicable to one extreme case where the tube is completely free to bend. In the opposite extreme case of total constraint against bending, a criterion based on maximum shear stress in the net section as proposed by Cochet et al.[15] can be used to calculate the instability limit pressure

$$p_{cr} = \frac{2(\gamma^2-1)(\pi-\theta)\overline{\sigma}}{2\pi+(\pi-\theta)(\gamma^2-1)} \tag{6a}$$

where

$$\gamma = \frac{R_o}{R} \tag{6b}$$

In reality, the tube support plates offer a significant but not total restraint against bending which tends to increase the rupture pressure to somewhere between those predicted by Eqs. 5a and 6a.

Hernalsteen[16] has developed a semi-empirical approach for taking into account the stiffening effects of the tube support plate on the burst pressure of a steam generator tube containing a circumferential crack at the top of the tube sheet. By conducting a number of burst tests of circumferentially precracked steam generator tube/tube sheet/tube support plate assembly and measuring the burst pressures p_{burst} as well as the restraining loads (thus the bending moments M_{burst} at the tubesheet) at the tube support plate at burst, he has developed an empirical correlation between the stress index K and the elastic rotational stiffness of the tube S, where

$$K = \frac{\left[\frac{M_{burst}}{\pi R_m^2 h} + \frac{p_{burst} R_m}{2h}\right]}{\overline{\sigma}} \tag{7a}$$

and

$$S = \frac{M}{EIy'}\ , \tag{7b}$$

EI the flexural stiffness of the tube, M and y' are the bending moment, and rotation at the tube sheet, respectively.

Based on this correlation, Hernalsteen has determined the value of K from the value of S that corresponds to the steam generator tube configuration under consideration and computed the burst pressure from Eq. 7a. Typical values of K ranged from 0.6 for 2-3 m span to 0.9 for 3-4 cm span between the tube sheet and the tube support plate.

A series of elastoplastic finite element analyses are being conducted at ANL to determine the effects of a lateral constraint on the burst pressure of a tube with a single through wall circumferential crack. Initially, two tubes with 180° and 240° through wall circumferential cracks have been analyzed. A typical finite element model and displacements for the free-bending case are shown in figs. 3 a-b. Note that the beam bends almost like a rigid body about a hinge at the cracked section. Fig. 4a shows the variations of the free-end displacements and the maximum rotation with the normalized burst pressure for a 180° and a 240° circumferential through wall cracks. The displacement and rotation curves coincide, confirming that the displacement is of the rigid-body-rotation type. Both cracked tubes reach maximum pressures at a rotation of ~ 10°. This is in agreement with the experimental observation by Hernalsteen[16] that tubes appear to fail at a fixed rotation of the cracked section. Fig. 4b shows a comparison between available burst pressure data reported by Cochet and Flesch[17] with predictions by the simple beam free-bending model (Eq. 5a) and finite element analysis. The simple model underpredicts the test burst pressures as well as the finite element results slightly. Preliminary analysis of a transversely supported (to simulate the tube support plate) tube with a 240° crack showed that the maximum pressure capability is increased significantly compared to that of a free-bending tube (fig. 5a). The critical pressure for a span of 0.67 m (26 in.) appears to be much closer to the fully constrained case than the free-bending case (fig. 5b).

High temperature failure of tubes

The behavior of flawed steam generator tubing during severe accidents has recently been considered in a report by INEL[7] and an EPRI report.[8] In these reports, the failure of unflawed tubing and other components such as the surge line nozzle was described in terms of creep damage failure. In contrast, both analyses assumed that failure of flawed (axial crack) steam generator tubing in severe accidents can be described in terms of the models described by Eqs 1–3 by taking the flow stress to be a function of temperature. With this assumption, the failure pressure of a flawed tube depended only on the flaw geometry and temperature and was independent of the detailed time/temperature/pressure history.

Recent tests conducted at ANL have shown that pressure and temperature ramp rates have significant influences on the failure pressure (fig. 6a) and failure temperature (fig. 6B), respectively. Therefore, a creep rupture model for predicting failure of flawed and unflawed tubes is developed in the present paper. Predictions based on this model for high temperature tests conducted at ANL under a variety of loading histories are much more in agreement with test results than those based on the flow stress models. However, for completeness, the flow stress models are also discussed in this paper.

Intuitively, failure would be expected to be controlled by flow stress if the temperature ramps are sufficiently rapid so that there is insufficient time for creep to influence the deformation or damage of the tube. At the other extreme, if the temperature ramps are sufficiently slow (in the limit, a constant temperature hold), failure should be controlled by creep processes. In loading histories at intermediate rates, the damage processes are more complex and difficult to analyze.

Consider a tube with a flaw subjected to a temperature history T(t) and nominal hoop stress history $\sigma(t)$. To analyze the behavior of a tube under such a general loading history, both the flow stress and the creep rupture models make the following assumptions:

(1) The failure time and temperature of a flawed tube are the same as those of an unflawed tube subjected to a nominal hoop stress history $m_p\sigma(t)$ and the same temperature history T(t).

(2) The values of the magnification factor m_p determined from burst tests of flawed tubes at low temperatures are also applicable at high temperatures.

These assumptions may be valid for certain classes of creep and plasticity problems.[18] They are not strictly valid for the problem considered here, but the test program at ANL has shown that they can provide a reasonable approximation.

Flow stress models

In the flow stress models, it is assumed that, for any arbitrary history of hoop stress $\sigma(t)$ and temperature T(t), rupture of the remaining ligament occurs at a temperature T and nominal hoop stress σ whenever the following rupture equation is satisfied, independent of stress-temperature history:

$$\sigma = \frac{\overline{\sigma(T)}}{m_p} \tag{8}$$

where $\overline{\sigma(T)}$ is the flow stress at temperature T and m_p is a model-dependent hoop stress magnification factor that accounts for the crack (see Eqs. 2-4). Conceptually, it is possible to include rate effects within the framework of a flow stress model by generalizing the constitutive equation so that the flow stress is a function of strain rate as well as temperature. In fact, several such constitutive relations based on the so-called equation of state theory are currently available (for example, see Ref. 19). However, in addition to being quite complex they are not easily amenable to the problem of predicting failure of steam generator tubes, particularly those that contain flaws and are subjected to typical temperature and pressure histories expected during a severe accident.

In this paper, the term flow stress models is used exclusively to denote simple rate-independent flow stress models. Because of their success at low temperatures, they were used initially with the hope that they would provide reasonable failure predictions for the high temperature tests provided the tests were conducted at sufficiently high loading rates. Flow stresses (computed with k=0.5) for Alloy 600 from various sources[6, 9, 20,21] are plotted in Fig. 7. Note that although there may be a wide variation in the flow stress at low temperatures, the product form variations in the flow stress diminish rapidly with increasing temperature. Therefore, the INEL flow stress curve, which covers the widest range of temperature, is used for failure predictions.

To evaluate the importance of loading rates on the failure conditions, two types of tests were conducted on unflawed steam generator tubes. First, the specimens were heated to a temperature and then pressurized isothermally at a constant pressure ramp until failure. In the second type of tests, the specimens were first pressurized at low temperature, and then, holding the pressure constant, they were subjected to a constant temperature ramp until failure. Results from both types of tests, plotted in figs 6a and 6b, clearly show that loading rates have significant effects on the failure conditions. In particular, the predictions by the flow stress model can be significantly off even for an unflawed tube. Therefore, it was concluded that a simple rate-independent flow stress model cannot be used reliably to predict failure under a varying temperature and pressure history expected during a severe accident.

Creep rupture model

Creep failure of a uniaxially loaded specimen under a varying stress and temperature history can be predicted by a relatively straight forward analysis[18], and is often based on a linear time-fraction damage rule (e.g., Code Case N 47 of the ASME Code, Section III), as follows:

$$\int_0^{t_f} \frac{dt}{t_R(T,\sigma)} = 1 \tag{9}$$

where t_R is the time to creep rupture for a uniaxial specimen under a stress σ and temperature T, both of which may be functions of time, and t_f is the time to failure.

To apply the creep rupture model for predicting failure under severe accident conditions, creep rupture properties (particularly at short lives) of Alloy 600 tubes in the hoop direction are needed. Available creep rupture data (uniaxial tests) from the literature were collected and the following Larson-Miller representation for the data was established[10]:

$$t_R = 10^{\frac{LMP}{T-15}} \tag{10a}$$

where T is in K and the Larson-Miller parameter LMP is defined in terms of the stress σ (in ksi) as follows:

$$LMP = \begin{cases} 23.14 - 2.4\log_e(\sigma) \text{ for } \sigma \geq 5.7\,\text{ksi} \\ 24.18 - 3.0\log_e(\sigma) \text{ for } \sigma < 5.7\,\text{ksi} \end{cases} \tag{10b}$$

To establish the applicability of Eqs. 10a-b to our tubing material, constant-pressure creep-rupture tests were conducted on unflawed 22 mm (7/8 in.) dia. tubes using both isothermal and constant temperature ramp loading. The experimental results are plotted in fig. 8 against predicted times to rupture, using Eqs. 10a-b. In all cases, the predicted rupture lives are well within a factor of 2 of the experimental lives, thus indicating that the above Larson-Miller representation of the data is adequate for our material.

Validation tests for the creep rupture model applied to flawed specimens

A rigorous analysis of flawed tubes under a similar loading would be very complex. Therefore, the creep failure model was extended to flawed tubing using the assumptions referred to earlier, i.e., it was assumed that failure can be predicted by the following equation:

$$\int_0^{t_f} \frac{dt}{t_R(T, m_p\sigma)} = 1 \tag{11}$$

To validate the above approach, rupture tests were conducted on flawed tubing subjected to isothermal constant pressure loading. The predicted failure times using four different values of m_p are plotted against the experimental failure times in fig. 9a for tubes containing a ~60% deep 25 mm (1 in.) long crack. Except for a test at 667°C, the predicted rupture lives by the ANL m_p (Eq. 2c) are within a factor of 2 of the experimental lives of the specimens. The predicted lives using m_p values as determined by the BCL (Eq. 2b) and EDF (Eq. 4a) equations are also reasonable, but those by the INEL equation (Eq.3b) are significantly off in most cases.

There is some experimental evidence[5] that indicates that the numerical values of m_p computed by the BCL equation for short and deep cracks are too high for tests conducted at low temperatures where a flow stress model is valid. Results from tests confirming that this is also a problem at high temperatures are shown in Fig. 9b. All the test specimens referred in this figure had ≥ 90% deep cracks. Note that the BCL equation grossly overestimates the damaging influence (i.e., underestimates the time to rupture) of these cracks. The INEL and ANL equations do account for the less damaging influence of the deeper cracks as compared to the shallower cracks. The predictions by the EDF equation are not shown in fig. 9b because at high temperatures, they are essentially the same as those by the BCL equation. This is so because Flesch and Cochet[5] have accounted for deep cracks that are more than 85% deep by replacing the flow stress in the BCL equation by the ultimate tensile strength, see Eq. 4b. However, because of a lack of strain hardening, there is little difference between the flow stress and the ultimate tensile strength at high temperatures. Consequently, the EDF equation fails to account for the less damaging influence of deep cracks at high temperatures. Overall, the ANL equation gives the best predictions for rupture lives of specimens with shallow as well as deep cracks and is used for predicting failure of the high temperature tests.

Prediction of rupture tests under simulated severe accident conditions

With the recently rising concern for severe accidents in PWR, the NRC has sponsored a series of tests at ANL to help develop and validate a model for predicting rupture of both flawed and unflawed steam generator tubes under such accidents. The tests were conducted by keeping the internal pressure constant at 16 MPa (2.35 ksi) and ramping the temperature according to two scenarios calculated by INEL[7] and EPRI[8], shown in figs. 10a and 10b, respectively. Both the 22 mm (7/8 in.) and the 19 mm (3/4 in.) tubes with axial cracks of length 6 mm (0.25 in.), 25 mm (1 in.), and 51 mm (2 in.) with crack depths varying between 20% and 65% were tested. The experimental temperatures and times to failure are compared with predicted failure temperatures and times in figs. 11a and 11b, respectively. The predicted values were calculated with the creep rupture model using the Larson-Miller parameter, Eq. 10a-b and stress magnification factor, Eq. 2c. In most cases, the predicted times and temperatures are quite close to the experimentally observed values.

Conclusions

Available flow stress models for predicting failure of flawed steam generator tubing under normal operating conditions and design basis accidents have been reviewed. All the models predict similar rupture pressure for shallow axial cracks, but give significantly different rupture pressures when the cracks are deep. A new correlation developed recently developed at ANL appear to correlate data for all flaw depths better than the existing ones. The new correlation is supported by detailed finite element analysis.

The failure pressure for tubes containing unsymmetrical circumferential cracks has recently been observed experimentally to increase in the presence of lateral constraint. Detailed finite element analyses show that such a behavior is to be expected and that a tube support plate spacing of 0.65 m (26 in.) or less should increase the rupture pressure to almost that of a fully constrained tube.

Rupture tests conducted at high temperatures expected during severe accidents show that the failure pressure at a constant temperature is dependent on the pressure ramp rate and the failure temperature at a constant pressure is dependent on the temperature ramp rate. A simple rate-independent flow stress model cannot predict such a behavior. A creep rupture model developed at ANL can predict such a behavior.

The creep rupture model, which uses the same m_p factor as that developed for a flow stress model at ANL, has been validated with isothermal rupture tests on specimens with cracks of various size. The model can predict failure of flawed and unflawed tubes subjected to a varying temperature and pressure history expected during severe accidents.

Acknowledgment

The author would like to acknowledge helpful discussions with Drs. W.J. Shack and D.R. Diercks of Argonne National Laboratory and Dr. J. Muscara of the U.S.N.R.C. Thanks are also due to Messrs. J. Franklin and L. Knoblich for conducting the high temperature rupture tests and to Mr. Keith Mruk for providing the measured crack parameters.

References

1. G.T. Hahn, M. Sarrate, and A.R. Rosenfield, "Criteria for crack extension in cylindrical pressure vessels," *Int. J. Fracture Mech.*, Vol. 5, No. 3, 1969.

2. F. Erdogan, "Ductile failure theories for pressurized pipes and containers," *Int. J. of Pres. Ves. & Piping*, Vol. **4**, 1976.

3. R. J. Eiber, W. A. Maxey, A. R. Duffy, and T. J. Atterbury, "Investigation of the Initiation and Extent of Ductile Pipe Rupture," BMI–1908, Battelle Memorial Institute, June 1971.

4. J. F. Kiefner, W.A. Maxey, R.J. Eiber, and A.R. Duffy, "Failure stress levels of flaws in pressurized cylinders," in *Progress in Flaw Growth and Fracture Toughness Testing*,, Kaufman, J. G., National Symposium on Fracture Mechanics (6th : 1972 : Philadelphia), American Society for Testing and Materials, Committee E–24 on Fracture Testing of Metals, American Society for Testing and Materials, ASTM Special Technical Publication 536, Philadelphia 1973.

5. B. Flesch and B. Cochet, "Crack stability criteria in steam generator tubes," *Int. Cong. on Pressure Vessel Technology*, Beijing, Sept. 1988.

6. R.J. Kurtz, R.A. Clark, L.R. Bradley, W.M. Bowen, P.G. Doctor, R.H. Ferris, and F.A. Simonen, *Steam Generator Tube Integrity Program/Steam Generator Group Project, Final Project Summary Report,* NUREG/CR–5117, PNNL, Richland, WA, May 1990.

7. P. G. Ellison, L. W. Ward, C. Dobbe. S. A. Chavez, C. L. Atwood, C. L. Smith, L. M. Wolfram, J. L. Jones, L. N. Haney, and W. J. Reece, The Risk Significance of Induced Steam Generator Tube Rupture, INEL-95/0641, Rev. 1 (Draft), Lockheed Martin Idaho Technologies, Inc., Idaho National Engineering Laboratory, December 15, 1995.

8. E. L. Fuller, M. A. Kenton, M. Epstein, R. E. Henry, and N. G. Cofie, Risks from Severe Accidents Involving Steam generator Tube Leaks or Ruptures, EPRI TR-106194, Electric Power Research Institute, Palo Alto, CA (to be published).

9. S. A. Chavez, C.L. Atwood, P.G. Ellison, and J.L. Jones, "Estimating structural failure frequency of degraded steam generator tubes", Submitted to ASME

10. W.J. Shack, Argonne National Laboratory, personal communication, 1996.

11. S. Ranganath and H. S. Mehta, "Engineering Methods for the Assessment of Ductile Fracture Margin in Nuclear Power Plant Piping," Elastic Plastic Fracture Second Symposium, Vol. 2, Fracture Resistance Curves and Engineering Applications, American Society for Testing and Materials, ASTM Special Technical Publication 803, Philadelphia 1973.

12. M. F, Kanninen, A. Zahoor, G. M. Wilkowski, I. Abou–Sayed, C. Marschall, D. Broek, S. Sampath, C. Rhee, J. Ahmad, "Instability Predictions for Circumferentially Cracked Type 304 Stainless Steel Pipes under Dynamic Loading," EPRI NP–2347 (Vol.1: Summary; Vol. 2: Appendices), Electric Power Research Institute, Palo Alto, CA, April 1982.

13. K. Hasegawa, T. Shimizu, and S. Shida, Consideration of Allowable Flaw Size for Pressurized Pipes, *Nucl. Eng. and Design*, Vol. 87, 1985.

14. R. Kurihara, S. Ueda, and Dietmar Sturm, Estimation of the Ductile Unstable Fracture of Pipe with a Circumferential Surface Crack subjected to Bending, *Nucl. Eng. and Design*, . Vol. 106, 1988.

15. B. Cochet, J. Engstrom, and B. Flesch, "PWR steam generator tube and tube support plate plugging criteria," Paper 4.1, *Steam generator tubes mechanical, LBRB, and probabilistic studies*, EDF, France.

16. P. Hernalsteen, "Structural and Leakage Integrity of Tubes Affected by Circumferential Cracking", presented at the NEA/CNRA/CSNI International Workshop on Steam Generator Integrity in Nuclear Power Plants, Oak Brook, Illinois, October 30-November 2, 1995.

17. B. Cochet and B. Flesch, "Application of the leak before break concept to steam generator tubes," SMIRT–9, Vol. D, Lausanne, 1987.

18. I. Finnie and W. R. Heller, *Creep of Engineering Materials,* New York, McGraw-Hill, 1959.

19. E.W. Hart, "A phenomenological theory for plastic deformation of polycrystalline metals", Acta Met., Vol. 18, 1970.

20. J. L. Rempe, S.A. Chavez, G.L. Thinnes, C.M. Allison, G.E. Korth, R.J. Witt, J.J. Sienicki, S.K. Wang, L.A. Stickler, C.H. Heath, and S. D. Snow, *"Light Water Reactor Lower Head Failure Analysis",* NUREG/CR-5642, EGG-2618, I.N.E.L, Idaho Falls, ID, October, 1993.

21 International Nickel Co., "Engineering Properties of Inconel Alloy 600", Tech. Bull. T-7, 1964.

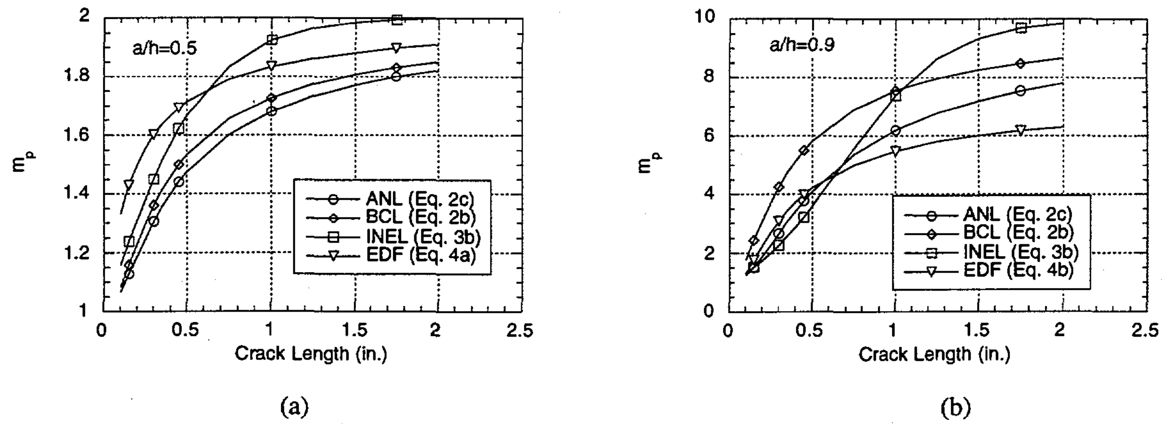

Fig. 1 *Magnification factor m_p as computed by the BCL (Kiefner et al.) equation (Eq. 2b), ANL (Shack) equation (Eq. 2c), INEL (Chavez et al.) equation (Eq. 3b), and the EDF (Flesch and Cochet) equation (Eqs. 4a-b) as a function of crack length for crack depth to thickness ratios (a) a/h=0.5 and (b) a/h=0.9.*

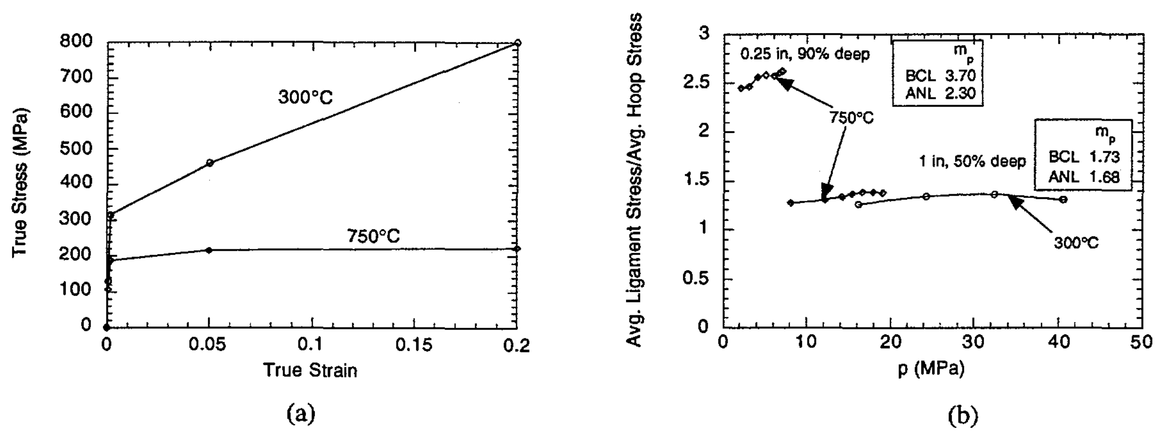

Fig. 2 *(a) True stress-strain curve used in the finite-element analysis and (b) variation of calculated hoop stress enhancement factor in the ligament with pressure for a 22 mm (7/8 in.) dia. tube for two axial part-through crack geometries at 300°C and 750°C.*

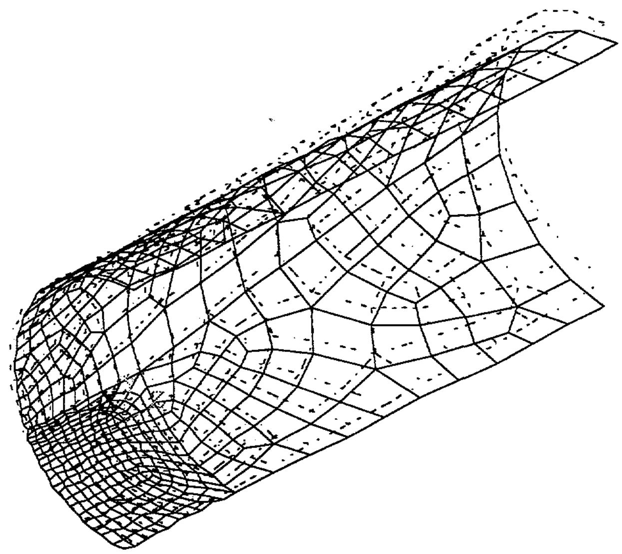

(a)

(b)

Fig. 3 *(a) Typical near-tip finite element model for a tube with a through wall circumferential crack. (b) Typical displaced shape of the tube for the free-bending case.*

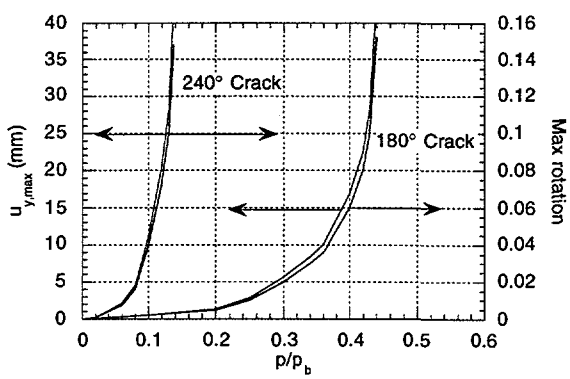

(a)

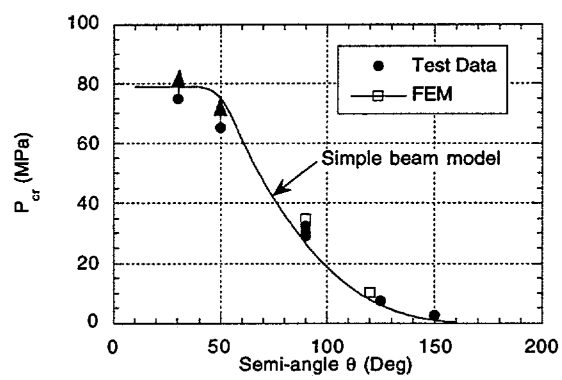

(b)

Fig. 4 *(a) Variations of free end displacements and maximum rotations with normalized burst pressure for tubes with 240° and 180° through wall circumferential cracks. (b) Comparison of experimental burst pressure data with predicted burst pressures using a simplified beam model and finite element method.*

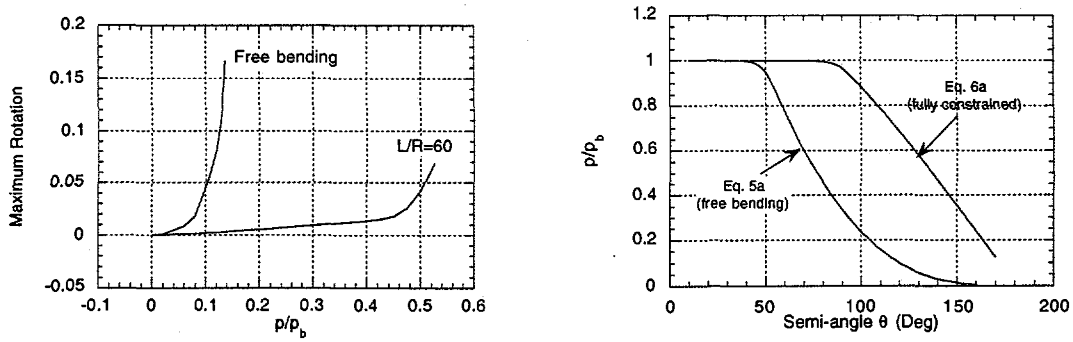

(a) (b)

Fig. 5 *(a) Maximum rotation of the section of a 22 mm (7/8 in.) dia. tube containing a 240° circumferential crack when it is free to bend and when it is supported laterally at a span of 0.67 m (26 in.) and (b) variation of critical burst pressure with semi-angle of crack for free-bending and fully constrained cases.*

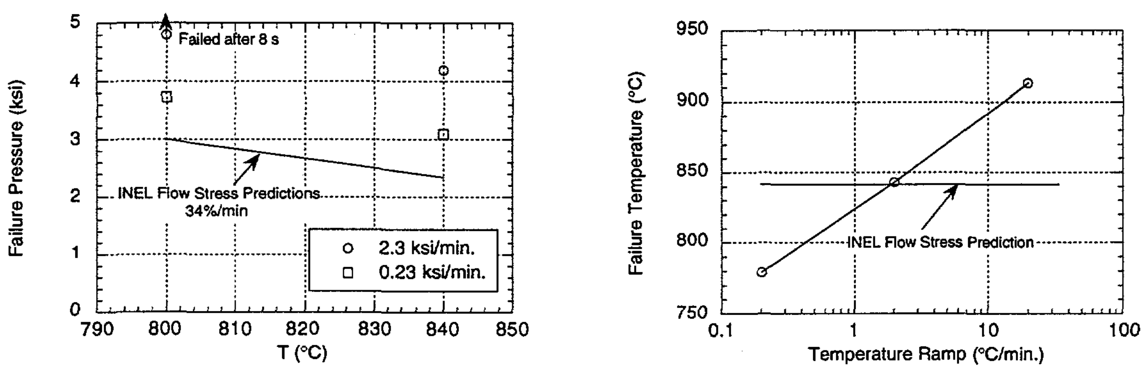

(a) (b)

Fig.6 *Effects of (a) loading rate on the failure pressure in an isothermal burst test and (b) temperature ramp on the failure temperature in a burst test at a constant pressure of 16 MPa (2.35 ksi) of an unflawed 22 mm (7/8 in.) dia. Inco 600 tube.*

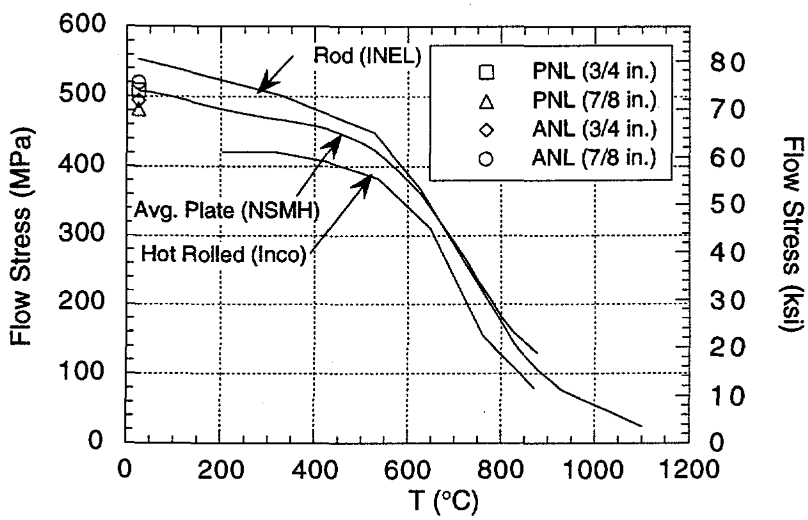

Fig. 7 *Flow stress for various product forms of Inco 600 as a function of temperature.*

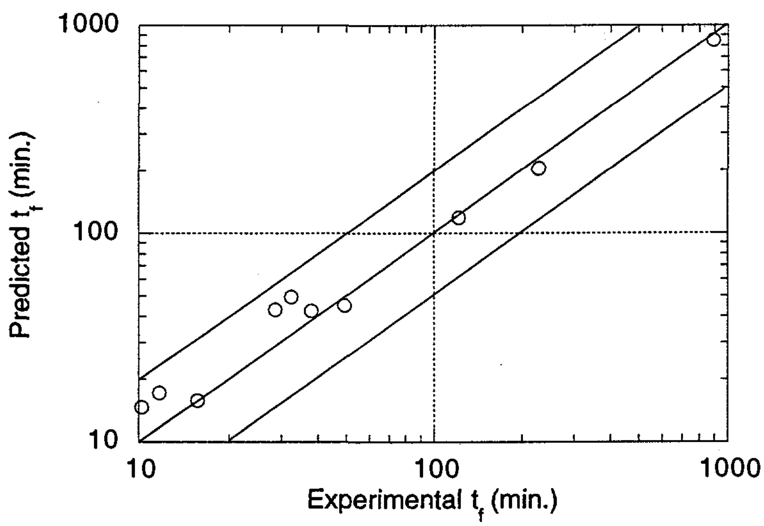

Fig. 8 *Comparison of experimental and predicted times to rupture of unflawed Inco 600 tubing under constant internal pressure. Tests were conducted isothermally and under constant temperature ramps of 0.2°C/min., 2°C/min., and 20°C/min.*

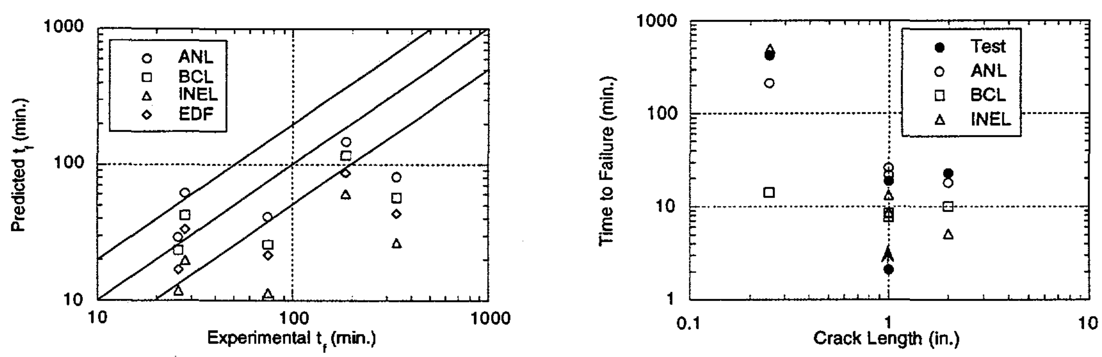

(a) (b)

Fig. 9 *Comparison of experimental and predicted times to rupture of flawed Inco 600 tubing tested isothermally under constant internal pressure, for (a) shallow flaws of length of 25 mm (1 in.) and depths varying between 56% to 65% and at temperatures varying between 667°C and 800°C and (b) deep flaws with depths varying between 90% and 92% at a temperature of 800°C. The arrow indicates a pin hole failure in which the pressure was undiminished after the failure, but the test was interrupted.*

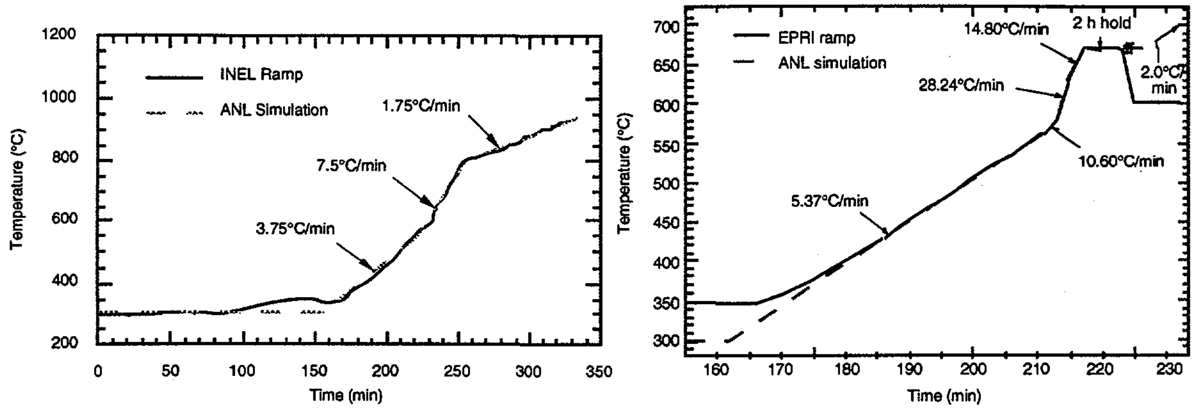

(a) (b)

Fig. 10 Calculated and ANL simulation of (a) INEL ramp and (b) EPRI ramp for the high temperature tests.

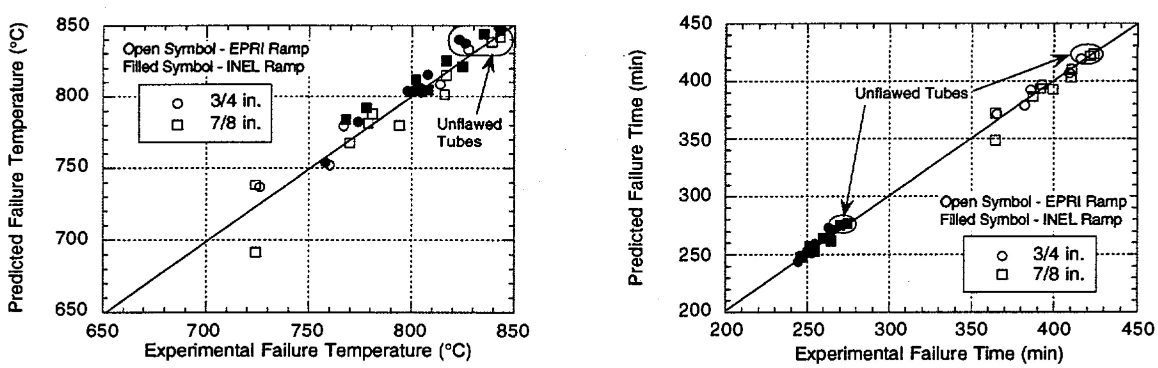

(a) (b)

Fig. 11 Comparison of predicted versus observed (a) failure temperatures and (b) times to failure for high temperature rupture tests conducted using the INEL temperature ramp and the EPRI temperature ramp.